



## The initial subevent of the 1994 Northridge, California, earthquake: Is earthquake size predictable?

D. Kilb<sup>1</sup> & J. Gomberg<sup>2</sup>

<sup>1</sup>*CERI, The University of Memphis, Memphis, TN 38152, U.S.A.*; <sup>2</sup>*U.S. Geological Survey and CERI, Memphis, TN 38152, U.S.A.*

Received 3 March 1998; accepted in revised form 20 January 1999

*Key words:* 1994 Northridge, California, earthquake; nucleation; precursor; seismology; waveform analysis

### Abstract

We examine the initial subevent (ISE) of the  $M_w$  6.7, 1994 Northridge, California, earthquake in order to discriminate between two end-member rupture initiation models: the ‘preslip’ and ‘cascade’ models. Final earthquake size may be predictable from an ISE’s seismic signature in the preslip model but not in the cascade model. In the cascade model ISEs are simply small earthquakes that can be described as purely dynamic ruptures. In this model a large earthquake is triggered by smaller earthquakes; there is no size scaling between triggering and triggered events and a variety of stress transfer mechanisms are possible. Alternatively, in the preslip model, a large earthquake nucleates as an aseismically slipping patch in which the patch dimension grows and scales with the earthquake’s ultimate size; the byproduct of this loading process is the ISE. In this model, the duration of the ISE signal scales with the ultimate size of the earthquake, suggesting that nucleation and earthquake size are determined by a more predictable, measurable, and organized process. To distinguish between these two end-member models we use short period seismograms recorded by the Southern California Seismic Network. We address questions regarding the similarity in hypocenter locations and focal mechanisms of the ISE and the mainshock. We also compare the ISE’s waveform characteristics to those of small earthquakes and to the beginnings of earthquakes with a range of magnitudes. We find that the focal mechanisms of the ISE and mainshock are indistinguishable, and both events may have nucleated on and ruptured the same fault plane. These results satisfy the requirements for both models and thus do not discriminate between them. However, further tests show the ISE’s waveform characteristics are similar to those of typical small earthquakes in the vicinity and more importantly, do not scale with the mainshock magnitude. These results are more consistent with the cascade model.

*Abbreviations:* ISE – Initial sub-event; SCSN – Southern California Seismic Network

### Introduction

Can the size of any earthquake be determined from only the beginnings of its seismograms? The answer to this controversial question, first posed by Brune in 1979, has significant implications for earthquake prediction and hazard mitigation. Herein we define an initial subevent (ISE) as a rupture that is: (1) seismically observable; (2) occurs within the initial ~16 percent of the total duration of the mainshock (Beroza and Ellsworth, 1996); and (3) the subevent with the greatest energy release yet has smaller magnitude than

the mainshock. ISEs form a small subset of foreshocks that encompass longer time intervals (days or weeks). ISEs have been observed in many studies, in recordings of micro-earthquakes (e.g., Iio, 1992 and 1995) and of small to large earthquakes in California and around the world (e.g., 1981 Gulf of Corinth, Greece (Abercrombie et al., 1995a), 1984 Western Nagano, Japan (Umeda, 1992); 1985 Michoacan, Mexico (Anderson and Chen, 1995); 1992 Landers, California (Abercrombie and Mori, 1994), 1994 Northridge, California (Beroza and Ellsworth, 1996); 1994 Romanche (McGuire et al., 1996); 1995 Ridgecrest,

California (Mori and Kanamori, 1996; Ellsworth and Beroza, 1998)). Hypotheses relevant to ISEs and the predictability of earthquake size have also been tested using theoretical models (e.g., Shibazaki and Matsu'ura, 1995; Singh et al., 1998; Steacy and McCloskey, 1998) and laboratory experiments (e.g., Ohnaka and Kuwahara, 1990). However, no consensus has been reached as to whether earthquake nucleation begins with an aseismic preparatory process in a region that scales with the earthquake's ultimate size, or as immediate dynamic rupture that simply continues until it is stopped by asperities and/or barriers. The details of these end-member processes, and whether they can be discriminated using observational data, also remain uncertain.

Recent work has attempted to distinguish between two end-member models that describe the relationship between an ISE and its mainshock: the cascade and preslip models. As in the studies listed above, we hypothesize that the ISE's waveform characteristics and parameters derived from them, can be used to discriminate between these end-member models. In the cascade model earthquake size is inherently unpredictable from the ISE's seismic waveform characteristics, whereas in the preslip model earthquake size may be predictable. The two models differ in the loading processes that give rise to the ISE. These processes manifest in different predictions of the ISE's seismic signatures.

In the cascade model earthquakes begin as dynamic failures without slow precursory slip. One earthquake provides the loading, or trigger, to initiate failure of another. The possible mechanisms responsible for the stress transfer are numerous; it may be via loading by coseismic static stress changes that concentrate at heterogeneities or crack-tips, dynamic stresses, or through changes in pore fluid pressures. In the immediate vicinity of the triggering earthquake the associated stress changes are most probably largest. Yet stress transfer mechanisms, such as dynamic stresses, may act over a greater distances ( $>1-2$  fault lengths), and may be more effective at triggering nucleation (Abercrombie and Mori, 1994; Abercrombie et al., 1995b). Thus, in the cascade model ISEs may occur on different fault planes and have different mechanisms than their mainshocks and, although perhaps not the most likely scenario, they need not occur close to their mainshock. This is contrary to the assumptions of Dodge et al. (1996) which considers triggering only via static stress transfer. Thus, the cascading earthquakes must occur close to, on the same plane, and

with the same mechanism as their mainshock. In this study we use a less restrictive definition. As we define it, in the general cascade model there are no location requirements or intrinsic scaling between the triggering (ISE) and triggered (mainshock) earthquakes. The triggering event acts only to initiate failure, and the size of the 'mainshock' event is ultimately determined by the distribution of heterogeneities that stop the rupture (Mori and Kanamori, 1996). There is also a specialized version of the cascade model, the hierarchical cascade model, in which the progression of triggering events grow in size as might occur if rupture propagation is controlled by a hierarchical distribution of faults.

In the preslip model earthquakes begin with slow precursory slip which is evident in ISE characteristics that scale with the mainshocks' size. The ISEs represent instabilities within a nucleation zone loaded by the surrounding aseismic slip. This creep occurs on an expanding fault patch, and the aseismically slipping area grows until the patch reaches a critical size when instability begins and rupture propagates or 'breaks away' (see Ellsworth and Beroza, 1995; Beroza and Ellsworth, 1996). This last stage of the rupture initiation process just prior to breakaway is termed the 'seismic nucleation phase'. In some of the observations described in Beroza and Ellsworth (1996) and others in Ellsworth and Beroza (1998), energy in this phase is released episodically and may be indistinguishable from that associated with a small earthquake, but then the release hesitates or slows down. If this is the case, ISE seismograms need not differ from seismograms of ordinary small earthquakes (modeled as simple immediate dynamic failure), except that they would exhibit a systematic scaling with mainshock moment. Ellsworth and Beroza (1998) suggest that the precursory events result as the aseismic slip creates localized stress concentrations that become unstable. Dodge et al. (1996) presents a similar model of foreshocks, stating that they are simply byproducts of this aseismic mainshock nucleation process. All these studies show a scaling between the nucleation phase or foreshock sequence duration and mainshock moment. The duration is presumed to represent the time required for the nucleation patch to grow to a critical size allowing breakaway. The longer the duration, the greater the accumulated slip in the nucleation zone, and the greater the 'push' available for the earthquake. Iio (1995) also measures a similar scaling, but his precursory observations have emergent beginnings that cannot be explained as simple dynamic

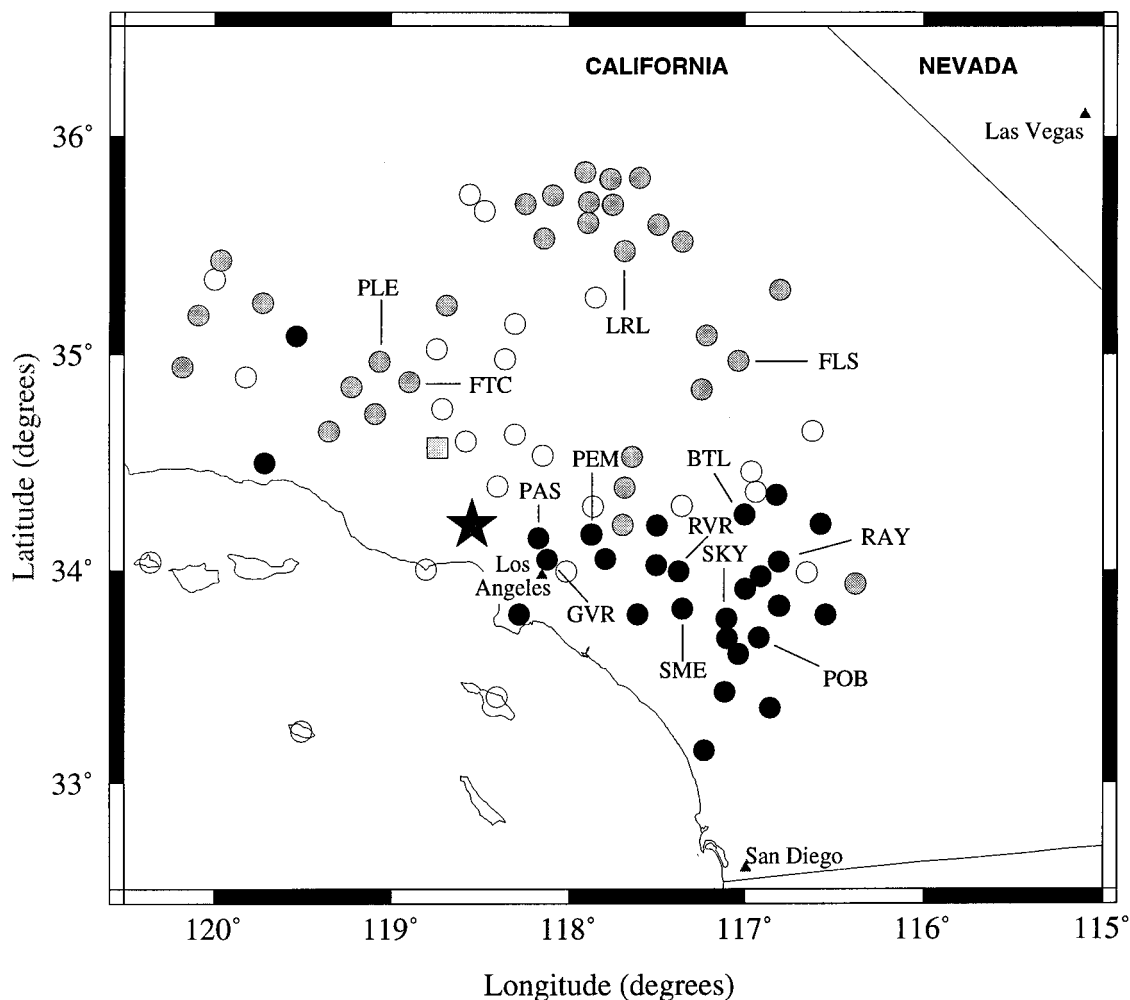


Figure 1. Locations of the mainshock hypocenter (star) and Southern California Seismic Network (operated by Caltech and USGS) seismic stations (circles and square) used in this study. Shading shows stations at which ISE and mainshock first motions are both up (black circles), both down (gray circles) and disagree (square). Stations providing additional data for time difference measurements (open circles) are also shown. Station names referred to in the text or other figures are labeled.

failures. Rather, they imply slow slip and/or rupture as in, for example, a slip-weakening crack model with longer ISE durations indicative of the longer time required to reach a slip-weakening distance. In the preslip model, whether an aseismically slipping patch or slip-weakening crack model is assumed, there is a nucleation phase with a duration that scales with mainshock moment.

The hierarchical cascade model, which satisfies the cascade model requirements, may also be consistent with observations indistinguishable from those predicted by the preslip model (Singh et al., 1998). However, the preslip model requires an additional mechanism for generating the appropriate delays between

triggering events so that the duration of the entire sequence scales systematically with the moment of the last and largest sub-event (the mainshock).

The location and rupture geometry of the ISE or foreshock may distinguish between the cascade and preslip models. The seismic nucleation phases studied by Ellsworth and Beroza (1995) are assumed to originate from the same fault as the corresponding mainshock, and the foreshocks studied in Dodge et al. (1996) most probably did also. The immediate proximity of the ISE to the mainshock location and the similar focal mechanisms seems consistent with the underlying loading process implicit in the preslip model. If the loading mechanism is stress localization

generated by the aseismic slip (or by slip-weakening crack-growth), then failure is most probably in the immediate vicinity of the slipping surface. These models do not consider stress transfer mechanisms, such as dynamic stresses, that act over any significant distance. ISEs that locate off the mainshock fault plane or have different mechanisms seem improbable if the preslip model is operative.

We attempt to discriminate between two end-member models (cascade and preslip) by addressing four questions using data from the 1994, Northridge, California,  $M_w$  6.7 mainshock and its associated ISE, as well as data from other smaller earthquakes in the vicinity. (1) Did the ISE occur on the mainshock rupture plane? A negative answer favors the general cascade model. (2) How similar are the focal mechanisms of the ISE and mainshock sources? Different mechanisms are more consistent with the general cascade model. (3) Does the Northridge ISE seismic signal differ from the beginnings of  $M$  6.7 earthquakes (i.e., do ISEs scale with mainshock size)? A negative answer indicates the cascade model is more plausible and an affirmative answer favors either the preslip or hierarchical cascade models. (4) Are the seismic waveform characteristics of the ISE similar to those of typical small earthquakes in the vicinity? An affirmative answer favors the cascade model, and a negative answer favors the preslip model.

## Data

We use seismograms of the Northridge earthquake recorded by the Southern California Seismic Network (SCSN). The SCSN stations are azimuthally and spatially well distributed (Figure 1), providing data well suited to test for differing ISE and mainshock locations and focal mechanisms. We use data from mostly high-gain stations (78) and where possible low-gain stations (11). These data are short-period seismograms recorded with a bandwidth of about 1–20 Hz, a dynamic range of  $\sim 40$ db, and sample rate of 100 Hz. Our analyses do not require any filtering, thereby eliminating the potential for filtering related artifacts. Without any processing these short period records show a clearly identifiable ISE signal that is distinct from the noise (Figure 2; Ellsworth and Beroza, 1995; Beroza and Ellsworth, 1996; Wald et al., 1996). The mainshock waveforms clip but this is of little concern because it is the fidelity of the ISE that is important in our study. Ellsworth and Beroza (1998) and

Mori and Kanamori (1996) also used clipped data, noting that these data are still useful for identifying characteristics of small precursory motions. We also use additional seismograms from other earthquakes ( $3.3 \leq M \leq 5.2$ ) that occurred in the same region as the Northridge mainshock. These permit us to examine ISEs of earthquakes of various sizes to determine if the scaling implicit in the preslip model exists.

## ISE and mainshock relative source locations

Our first objective is to determine if the Northridge ISE occurred on the mainshock rupture plane. We begin by determining bounds on the separation between the hypocenters of the ISE and mainshock sources by measuring the time difference,  $\Delta t$ , between their respective  $P$ -wave arrival onsets. The ISE's  $P$ -wave arrival is easily identified, and we assume the mainshock  $P$ -wave arrives when the seismogram first goes off scale. This only approximates the true mainshock arrival time, which probably occurs somewhere before the signal clips in the vicinity of the prior zero crossing. This introduces an average uncertainty of  $\sim 0.05$  seconds in our  $\Delta t$  estimates. To further check our assumed mainshock arrival times we compare, where available, low- and high-gain records recorded at the same stations (Figure 3). Crude conservative bounds on the relative locations of the ISE and mainshock hypocenters are obtained from the distribution of  $\Delta t$ s. The mean  $\Delta t$  of 0.5 seconds constrains the difference in ISE and mainshock origin times and the maximum  $\Delta t$  of 1 second provides a conservative upper bound of  $\sim 6$  km on their separation (assuming a  $P$ -wave velocity at the source from the rock model of Wald et al. (1996)). The azimuthal variation in  $\Delta t$  indicates that the ISE initiated up-dip of the mainshock hypocenter (Figure 4).

Similar to the work of Abercrombie and Mori (1994) we employ a grid-search fitting procedure to obtain a more precise estimate of the relative ISE source location. We compute relative travel-times by tracing rays through a plane-layered velocity model of the region (rock model; Wald et al., 1996). We determine location confidence regions based on a chi-squared statistic and an  $f$ -test distribution (Abramowitz and Stegun, 1972). Results for a plane coincident with the mainshock rupture surface and also a volume surrounding it show that the ISE source may have occurred on the mainshock rupture plane, up-dip and within 4 km of the mainshock hypocenter, with 0.5

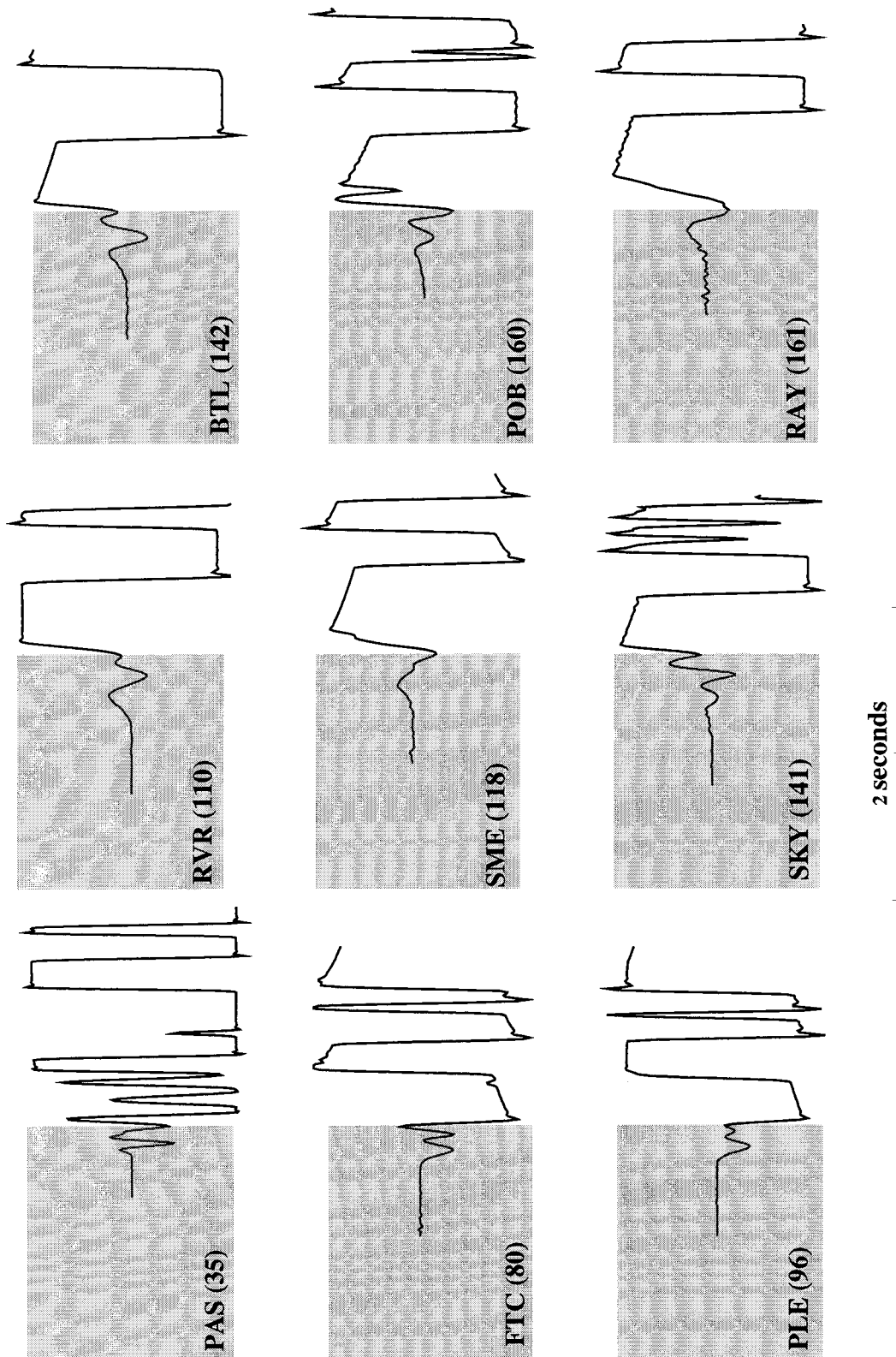


Figure 2. A small subset of the ISE seismograms of the 1994, Northridge, California, earthquake. The gray box differentiates the ISE from the mainshock signal. All waveforms were recorded on Southern California Seismic Network short period stations. Also listed are the station name and in parentheses, the source-station epicentral distance in kilometers.

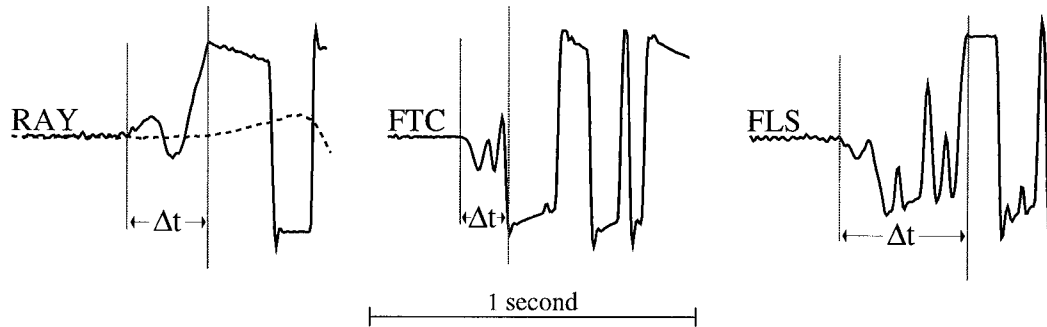


Figure 3. The time difference,  $\Delta t$ , between the ISE arrival (left vertical line) and the mainshock arrival (right vertical line). We assume that the first motion on the high-gain trace (solid line) is the arrival of the ISE, and that the mainshock energy arrives when the signal first clips. Low-gain traces where available (dashed line), validates this latter assumption. Also shown are examples where the ISE and mainshock first motions are both up (station RAY, left), both down (station FTC, center), and opposite (only at station FLS, right). The distances to stations RAY, FTC and FLS are 161, 80 and 162 km, respectively.

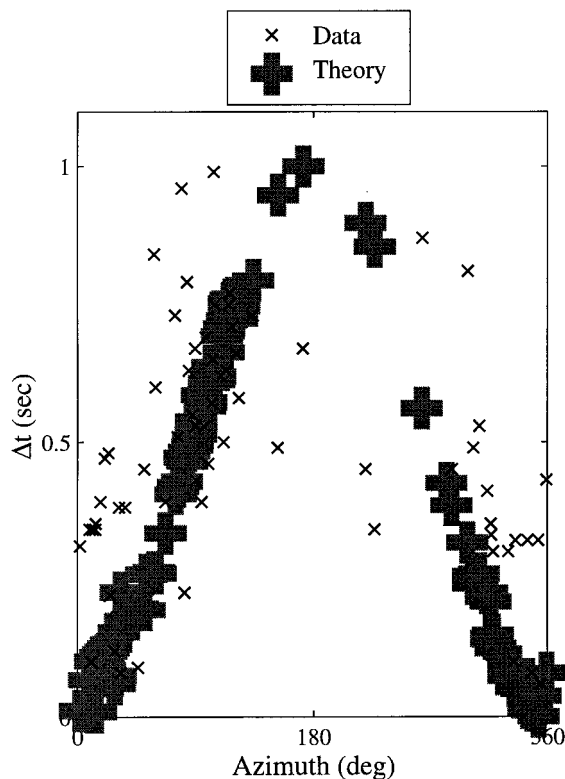


Figure 4. Time differences,  $\Delta t$ , between the ISE arrival and the mainshock arrival as a function of azimuth. Also shown are theoretically computed time lags from a ray tracing algorithm using an appropriate velocity model (Wald et. al., 1996, rock model) in which the ISE source location is located updip of the mainshock hypocenter.

seconds between origin times. The distance between ISE and mainshock hypocenters is probably less than 4 km. This reasonably assumes a rupture velocity of  $<3.6$  km/sec (shear velocity at the source (Wald et al., 1996)) which implies a separation of  $<1.8$  km given the estimated origin time difference. The close proximity of the ISE and mainshock do not allow us to rule out the possibility that they might both have occurred on the same fault plane. Consequently, this test fails to discriminate between the cascade and preslip models.

#### ISE/mainshock focal mechanisms

We initially evaluate the similarity of the ISE and mainshock focal mechanisms by comparing first motions of the ISE and mainshock signals. Of the 58 stations where first motions of both were identified, they differ at one station only (Figures 2 and 3). Although this suggests similar focal mechanisms, we test how different they might be by estimating the range of possible mechanisms consistent with the observations using the program FPFIT (Reasenber and Oppenheimer, 1985). Using first motions alone, without relative amplitude information, we find the fault plane parameters of the ISE (strike =  $135^\circ$ , dip =  $35^\circ$  and slip =  $130^\circ$ ) and mainshock (strike =  $145^\circ$ , dip =  $35^\circ$  and slip =  $140^\circ$ ) agree to  $\pm 10^\circ$ , which is within the calculated errors. These values differ somewhat from various published fault plane parameters of the Northridge mainshock, which use more data and/or more resilient methods that incorporate full waveform information (e.g. strike =  $122^\circ$ , dip =  $40^\circ$  and slip =  $101^\circ$  (Wald et al., 1996)). Although our observations

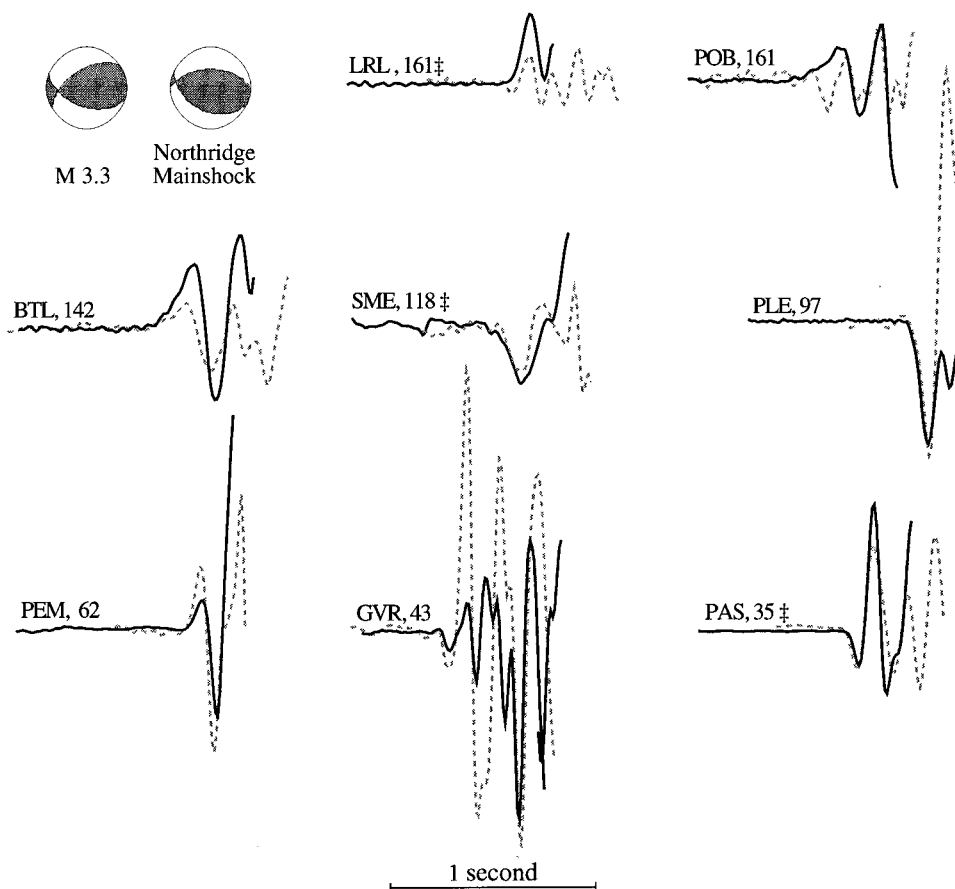


Figure 5. Comparison of short period seismograms for the Northridge ISE (solid) and a  $M$  3.3 earthquake (dashed). Focal mechanisms are also shown. Name, number and ‡ indicate station code, distance from mainshock and polarity reversal (consistent with focal mechanism differences) respectively.

do not adequately constrain the absolute focal mechanism parameters, they are sufficient to demonstrate that there is minimal difference between the ISE and mainshock mechanisms. We conclude that ISE and mainshock focal mechanisms are similar and possibly identical, which again fails to distinguish between the cascade and preslip models.

### ISE waveform characteristics and scaling

Guided by previous studies, we compare the Northridge ISE's waveform with waveforms from other earthquakes in the same area recorded at the same station (e.g., see Abercrombie and Mori, 1994; Anderson and Chen, 1995). We assume, as others have, that any variations between the waveforms reflect differences in source characteristics because of the similarity in

focal mechanisms, travel path, instrument response, and local site effects (Mori and Kanamori, 1996). The ISE's waveform characteristics (duration and amplitude) are consistent with dynamic rupture; i.e., they are very similar to those of a nearby  $M$  3.3 earthquake in the region (Figure 5). (Abercrombie and Mori (1994) make a similar comparison in their study of the Landers ISE earthquake.) This similarity suggests that a slip-weakening crack growth model as proposed by Iio (1995) is not appropriate unless the seismic energy it produces is in a frequency passband outside of the SCSN bandwidth. The similarity alone does not distinguish between the preslip and cascade model, although the later is perhaps more consistent with Occam's razor (i.e., does not require additional processes that cannot be observed). As discussed below, the waveform similarity combined with a lack of apparent scaling favors the cascade model.

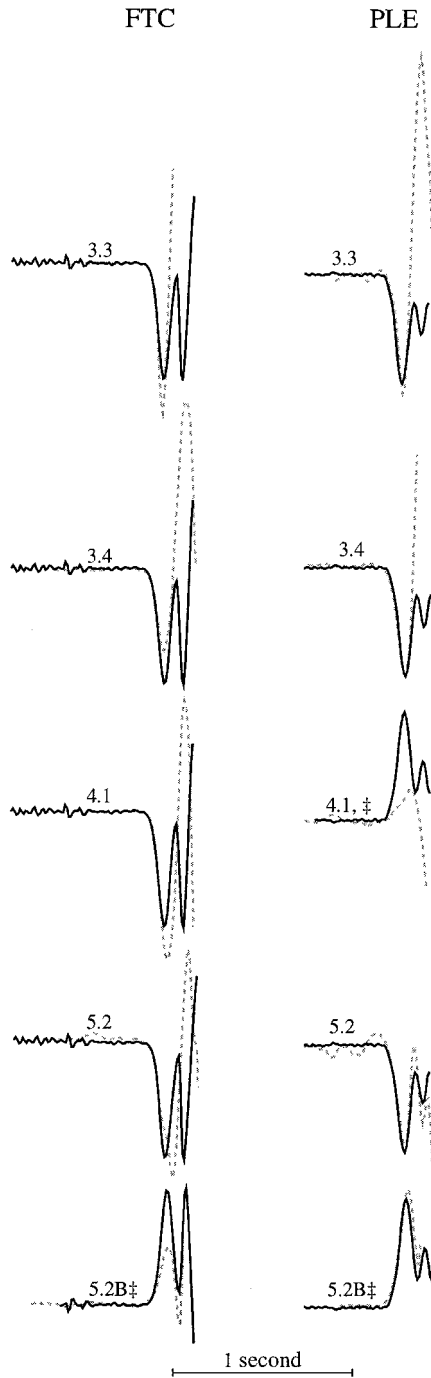


Figure 6. Waveform comparisons at stations FTC (left) and PLE (right) of the  $M_w$  6.7 Northridge ISE (solid) and those of smaller earthquakes in the same region (dashed). Numbers indicate magnitude of the small earthquake and ‡ indicates polarity reversal (consistent with focal mechanism differences). Waveforms in the last row come from earthquakes that were also used in other ISE studies (Ellsworth and Beroza, 1995; Beroza and Ellsworth, 1996). Stations FTC and PLE are a distance of 80.1 km and 96.8 km from the mainshock, respectively.

Most importantly, the Northridge ISE's waveform characteristics (duration and amplitude) do not scale with mainshock moment and cannot be distinguished from those of other earthquakes in the area. If scaling exists, the Northridge ISE waveform characteristics would only be similar to the beginnings of other  $M_w$  6.7 earthquakes and not to those of smaller or larger magnitude earthquakes. Such scaling should be apparent in unprocessed seismograms if it exists in this passband (Ellsworth and Beroza, 1995; Beroza and Ellsworth, 1996). We examine seismograms in which the first arrival is the direct  $P$ -wave (Vetter and Minster, 1981; Hearn, 1984; Hearn and Clayton, 1986; Hearn, 1996). The beginnings of the Northridge ISE seismograms are nearly identical to those of seismograms of five other earthquakes spanning a magnitude range of 3.3–5.2 (Figure 6). This indicates that the ISEs' waveform characteristics do not scale with mainshock moment. We cannot rule out the possibility that these waveforms would become more dissimilar at lower frequencies and scaling become apparent outside the instrumental bandwidth. However, in their studies of ISEs, Mori and Kanamori (1996) and Ellsworth and Beroza (1998) used data with comparable magnitude range and bandwidth to ours. The latter study finds evidence for scaling, suggesting it should be observable if it exists, even given this narrow bandwidth. Thus, the evidence we present favors the cascade model.

#### Possible sources of 'apparent' scaling

Our results are consistent with a number of recent studies which favor the cascade model (Bak and Tang, 1989; Umeda, 1992; Abercrombie and Mori, 1994; Abercrombie et al. 1995a, b; Anderson and Chen, 1995; Abercrombie and Mori, 1996; Mori and Kanamori, 1996; Steacy and McCloskey, 1998). These conclusions are based on various types of studies: cellular automata modeling, observations of unprocessed seismogram data, and Greens function deconvolution analyses. Other studies that favor the preslip model (Iio, 1992; Ellsworth and Beroza, 1995; Iio, 1995; Shibasaki and Matsu'ura, 1995; Beroza and Ellsworth, 1996) are also based on a number of different types of analyses: theoretical modeling, analysis of micro-earthquake data, and Greens function deconvolutions.

The set of earthquakes in our study overlaps with that analyzed by Ellsworth and Beroza (1995) and

Beroza and Ellsworth (1996) yet their conclusion differs from ours. Previously proposed explanations that may account for this difference are the bandwidth variations in which the studies were done (Abercrombie and Mori, 1994), or a consequence of attenuation (Singh et al., 1998). Additionally, we hypothesize that this difference may be a result of an apparent scaling that exists because the ISE, by definition, must be smaller than the mainshock and because larger earthquakes have longer source time functions. For example, the set of ‘possible’ ISE’s for a  $M$  6 earthquake includes all  $M < 6$  events, whereas only a subset of these are contained in the set of ‘possible’ ISEs for a  $M$  4 mainshock (i.e.  $M < 4$  events). Thus, the most probable ISE duration (source time function) will be longer for larger magnitude mainshocks.

Use of on-scale data may also lead to an apparent scaling because recording systems have limited dynamic and linearity ranges. (Linearity is the difference between the largest and smallest signals that can be identified in a single signal; it is usually smaller than the dynamic range.) For example, a system with 76 db linearity (equal to the dynamic range of a 16 bit system with 10 counts of noise) would be able to resolve on-scale signals from two nearly simultaneous events (ISE and mainshock) differing in magnitude by no more than 3.8 units. Thus, the observable ISE source size is bounded both above (it must be smaller than the mainshock) and below (by the recording system) which may contribute to an apparent scaling relationship. We do not suggest these affects completely explain ISE scaling but that they should be considered in interpretations.

Another possible contribution to apparent scaling may be the way data are processed. In our study, as in others, we assume that differences in source characteristics are evident in direct comparisons of waveforms with similar focal mechanisms, travel paths, instrument response, and local site effects (Mori and Kanamori, 1996). Other researchers that use data without these commonalties have attempted to remove the nonsource affects to obtain estimates of the source characteristics from individual seismograms. For example, support for scaling in most studies comes from moment-rate functions obtained by deconvolving small earthquake instrument-corrected seismograms or theoretical Green’s functions from instrument-corrected seismograms (e.g.,  $M > 4$  earthquakes in Ellsworth and Beroza, 1995; Beroza and Ellsworth, 1996). Although these studies appropriately deal with random error by optimizing decon-

volution trade-offs and checking the final fit to the data they may not preclude the possibility of systematic bias in the moment-rate function estimates (Sipkin and Lerner-Lam, 1992; Gurrola et al., 1995; Mori, 1996). Often solutions to deconvolutions are non-unique, varying significantly in the presence of small errors in the data or Green’s functions (Press et al., 1986; Dreger, 1994; Beroza and Ellsworth, 1996). Ultimately the solution depends on the implemented regularization method and, consequently, a number of moment-rate functions may produce equally good fits to the data with no guarantee that the one determined is not a biased representation of the true function. We do not imply that all observed scaling is a result of such bias, but merely point out the possibility is difficult to rule out.

We perform simple tests using synthetic data to determine if moment rate functions may be systematically biased. We generate synthetic data using a reflectivity method (Kennett, 1983; Randall and Taylor, 1993) with a one-layer earth model appropriate for our dataset (Wald et al., 1996). We first show that deconvolutions with Green’s functions that do not accurately model the true Earth structure may produce spurious ISE-like waveforms that scale with earthquake magnitude. The waveforms in our example have no noise or filtering, enabling us to produce accurate results using a simple frequency-domain spectral division deconvolution (i.e., no smoothing, tapering, filtering, or water-level cut-offs are used). We use triangular source functions to simulate moment-rate functions. Triangles with durations from 0.2 to 2.0 seconds, corresponding to earthquakes of  $M$  4.0 to  $M$  7.0, are convolved with noise-free point-source synthetic Green’s functions. A synthetic Green’s function computed with a source depth that is 2.5 km too shallow is deconvolved from the simulated larger earthquake seismograms. Recovered triangles have ISE-like artifacts with durations that increase with triangle width (Figure 7(a) and (b)), or equivalently mainshock magnitude. A comparable systematic bias also results for a source that is 2.5 km too deep. As shown in Figure 7(b), the apparent scaling relationship is similar to that found in other studies (Ellsworth and Beroza, 1995; Singh et al., 1998). Similar artifacts are produced when the  $P$ -wave velocity of the medium is either 2% too fast or too slow (Figure 7(b)). Although it is known that deconvolution stabilized using ‘waterlines’ causes artifacts, for completeness we verified this using exact deconvolved Green’s functions and found that indeed precursors that scaled with main-

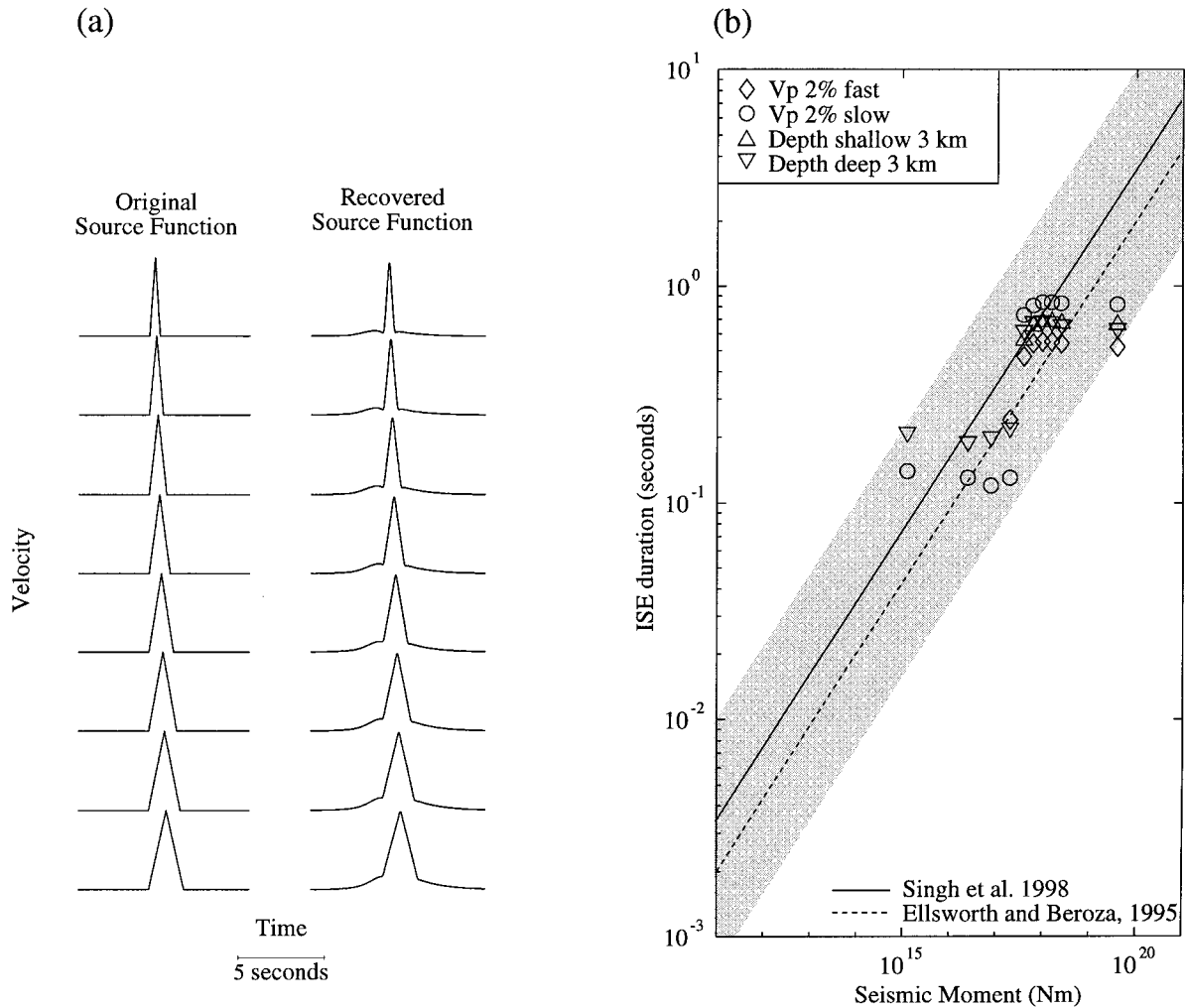


Figure 7. (a) Triangular source-time functions (left) with varying durations representing moment-rate functions of earthquakes with magnitudes ranging from  $M$  4 to  $M$  7. Each of these triangles are convolved with the same synthetic Greens function. Recovered source-time functions (right) are obtained by deconvolving a synthetic Greens function computed identically as that used to generate the input except that the source depth is 2.5 km shallower. Note the recovered triangles now have erroneous precursory signals that have durations that scale with the width of the input triangle. (b) Scaling relationship between mainshock seismic moment and the duration of the ISE signal. Results are shown from the deconvolution experiment described in (a) as well as other similar ones in which the deconvolved Greens function differed slightly from that used in the input; deconvolved Greens functions were calculated using  $P$ -wave velocity structure that was 2% too fast (diamonds), 2% too slow (circles), and for a source depth 2.5 km too deep (inverted triangles). The scaling relationships inferred in Ellsworth and Beroza, 1995 (dashed line) and Singh et al. 1998 (solid line) are also shown, and the shaded region roughly outlines the scatter in the data (Ellsworth and Beroza, 1995; Singh et al., 1998).

shock moment (triangle duration) resulted. In all these tests the residual between the input and predicted data is negligible.

In summary, these examples do not demonstrate that the ISE waveform scaling with mainshock moment inferred in other studies is necessarily a processing artifact; this was not our purpose and is beyond the scope of our study. Instead, we simply suggest

that data recording, selection, and processing all may contribute, to some degree, to apparent scaling.

## Conclusions

Our goal was to distinguish between the cascade and preslip models by comparing mainshock and ISE locations, focal mechanisms and waveforms. The

1994, Northridge, California, ISE and mainshock focal mechanisms are indistinguishable and both events could have nucleated on and ruptured the same fault plane. These results fail to discriminate between the cascade and preslip models. However, the Northridge ISE's waveform characteristics do not appear to scale with the mainshock size as the Northridge ISE waveforms are nearly identical to the beginnings of other earthquakes with magnitudes ranging from  $M$  3.3 to  $M$  5.2. The Northridge ISE's waveforms also are indistinguishable from those of typical small earthquakes in the vicinity. The combination of these observations are most consistent with the cascade model.

### Acknowledgements

We thank R. Abercrombie, J. Mori, B. Shibazaki, G. Beroza, and two anonymous reviewers for their thoughtful and insightful reviews. Valuable discussions with B. Ellsworth and G. Beroza were much appreciated. This work would not have been possible without the data provided by the Southern California Earthquake Center Data Center and the Southern California Seismic Network and the generosity of K. Hafner. We would also like to thank Paul Rydelek for assisting us with statistical tests. DK was partially supported by the Palisades Fellowship. CERI contribution number 338.

### References

- Abercrombie, R. and Mori, J., 1994, Local observations of the onset of a large earthquake: 28 June 1992 Landers, California, *Bull. Seis. Soc. Am.* **84**, 725–734.
- Abercrombie, R.E., Main, I.G., Douglas, A. and Burton, P.W., 1995a, The nucleation and rupture process of the 1981 Gulf of Corinth earthquakes from deconvolved broad-band data, *Geophys. J. Int.* **120**, 393–405.
- Abercrombie, R., Agnew, D. and Wyatt, F., 1995b, Testing a model of earthquake nucleation, *Bull. Seis. Soc. Am.* **85**, 1873–1878.
- Abercrombie, R. and Mori, J., 1996, Occurrence patterns of foreshocks to large earthquakes in the western United States, *Nature* **381**, 303–307.
- Abramowitz, M. and Stegun, A., 1972, *Handbook of Mathematical Functions* (9th edn), Dover Publications Inc., New York, N.Y.
- Anderson, J.G. and Chen, Q., 1995, Beginnings of earthquakes in the Mexican subduction zone on strong-motion accelerograms, *Bull. Seis. Soc. Am.* **85**, 1107–1115.
- Bak, P. and Tang, C., 1989, Earthquakes as a self-organized critical phenomenon, *J. Geophys. Res.* **94**, 15635–15637.
- Beroza, G.C. and Ellsworth, W.L., 1996, Properties of the seismic nucleation phase, *Tectonophysics* **261**, 209–277.
- Brune, J.N., 1979, Implications of earthquake triggering and rupture propagation for earthquake prediction based on premonitory phenomena, *J. Geophys. Res.* **84**, 2195–2198.
- Dodge, D.A., Beroza, G.C. and Ellsworth, W.L., 1996, Detailed observations of California foreshock sequences: Implications for the earthquake initiation process, *J. Geophys. Res.* **101**, 22371–22392.
- Dreger, D.S., 1994, Empirical Green's function study of the January 17, 1994 Northridge, California earthquake, *Geophys. Res. Lett.* **21**, 2633–2636.
- Ellsworth, W.L. and Beroza, G.C., 1995, Seismic evidence for an earthquake nucleation phase, *Science* **268**, 851–855.
- Ellsworth, W.L. and Beroza, G.C., 1998, Observation of the seismic nucleation phase in the Ridgecrest, California, earthquake sequence, *Geophys. Res. Lett.* **25**, 401–404.
- Gurrola, H., Baker, G.E. and Minster, J.B., 1995, Simultaneous time-domain deconvolution with application to the computation of receiver functions, *Geophys. J. Int.* **120**, 537–543.
- Hearn, T.M., 1984, Pn travel times in Southern California, *J. Geophys. Res.* **89**, 1843–1855.
- Hearn, T.M. and Clayton, R.W., 1986, Lateral velocity variations in southern California. II. results for the lower crust from Pn waves, *Bull. Seis. Soc. Am.* **76**, 551–520.
- Hearn, T.M., 1996, Anisotropic Pn tomography in the western United States, *J. Geophys. Res.* **101**, 8403–8414.
- Iio, Y., 1992, Slow initial phase of the P-wave velocity pulse generated by microearthquakes, *Geophys. Res. Lett.* **19**, 477–480.
- Iio, Y., 1995, Observations of the slow initial phase generated by microearthquakes: implications for earthquake nucleation and propagation, *J. Geophys. Res.* **100**, 15333–15349.
- Kennett, B.L.N., 1983, *Seismic Wave Propagation in Stratified Media*, Cambridge University Press, Cambridge.
- McGuire, J., Ihmle, P. and Jordan, T., 1996, Time-domain observations of a slow precursor to the 1994 Romanche transform earthquake, *Science* **274**, 82–85.
- Mori, J., 1996, Rupture directivity and slip distribution of the  $M$  4.3 Foreshock to the 1992 Joshua Tree Earthquake, Southern California, *Bull. Seis. Soc. Am.* **86**, 805–810.
- Mori, J., and Kanamori, H., 1996, Initial rupture of earthquakes in the 1995 Ridgecrest, California sequence, *Geophys. Res. Lett.* **23**, 2437–2440.
- Ohnaka, M. and Kuwahara, Y., 1990, Characteristic features of local breakdown near a crack-tip in the transition zone from nucleation to unstable rupture during stick-slip shear failure, *Tectonophysics* **175**, 197–220.
- Press, W.H., Flannery, B.P., Teukolsky, S.A. and Vetterling, W.T., 1986, *Numerical Recipes: The Art of Scientific Computing*, Cambridge University Press, Cambridge.
- Randall, G.E. and Taylor, S.R., 1993, Description of a code for computing complete synthetic seismograms in laterally homogeneous layered media.
- Reasenber, P. and Oppenheimer, D., 1985, FPFIT, FPLOT and FPPAGE: FORTRAN computer programs for calculating and displaying earthquake fault-plane solutions, U.S.G.S. Open File Report, 85-739, 109.
- Shibazaki, B. and Matsu'ura, M., 1995, Foreshocks and pre-events associated with the nucleation of large earthquakes, *Geophys. Res. Lett.* **22**, 1305–1308.
- Singh, S.K., Ordaz, M., Mikumo, T., Pacheco, J., Valdes, C. and Mandal, P., 1998, Implications of a composite source model and seismic-wave attenuation for the observed simplicity of small earthquakes and reported duration of earthquake initiation phase, *Bull. Seis. Soc. Am.* **88**, 1171–1181.

- Sipkin, S.A. and Lerner-Lam, A.L., 1992, Pulse-shape distortion introduced by broadband deconvolution, *Bull. Seis. Soc. Am.* **82**, 238–258.
- Steady, S.J. and McCloskey, J., 1998, What controls an earthquake's size? Results from a heterogeneous cellular automaton, *Geophys. J. Int.* **133** (1998), F11–F14.
- Umeda, Y., 1992, The bright spot of an earthquake, *Tectonophysics* **211**, 13–22.
- Vetter, U. and Minster, J.-B., 1981, Pn Velocity anisotropy in southern California, *Bull. Seis. Soc. Am.* **71**, 1511–1530.
- Wald, D.J., Heaton, T.H. and Hudnut, K.W., 1996, The slip history of the 1994 Northridge, California, Earthquake determined from strong-motion, teleseismic, GPS and leveling data., *Bull. Seis. Soc. Am.* **86**, S49–S70.